Induced Magnetic Properties of BN Nanotubes by the Adsorption of First-row Adatoms: An *ab initio* Study

**Fayyaz Hussain[1], Muhammad Imran[2]*, Nimra Fatima[1], Anwar Manzoor Rana[1]*,
R. M. Arif Khalil[1], Arshad Javid[3], and Muhammad Ismail[4]**

[1]*Materials Simulation Research Laboratory (MSRL), Department of Physics, Bahauddin Zakariya University Multan Pakistan, 60800*
[2]*Department of Physics, Govt. College University Faisalabad, Pakistan*
[3]*Department of Basic Sciences (Physics), University of Engineering & Technology, Taxila, Pakistan*
[4]*State Key Laboratory of Optoelectronic Materials and Technologies, School of Materials Science and Engineering,
Sun Yat-Sen University, Guangzhou 510275, China*

This work is performed to study the effect of adsorption of various first row adatoms (such as Be, C, F, Li and O) on (8, 0) zigzag boron nitride nanotubes (BNNTs) on their structural, electronic and magnetic properties. These calculations are based on density functional theory using pseudopotentials technique. For this purpose, five different sites namely axial, hexagonal, zigzag, on top of N and/or B (which are the most preferred available sites for adatoms on (8, 0) BNNTs) were utilized. The energetically stable sites for each of the first-row adatoms are found to be different because of their different electronic configurations caused by the charge transfer/ rearrangements between *s-p* or *p-p* orbitals. The binding energies of all adatoms on (8, 0) BNNTs have been calculated through structural optimization process after adsorbing these five adatoms at the above said sites on the BNNTs and are found to be in the energy range from −2.04 to 2.96 eV. It is further elaborated that F, Be and C adatoms on (8, 0) BNNTs show strong induced magnetization at specific localized sites depending upon the nature of adatom, whereas weak magnetization is noticed for Li and O adatoms on the BNNTs. Such localized induced magnetization could be associated with the hybridization of *s-p* or *p-p* orbitals of adatoms and B and/or N atoms.

Keywords : pseudopotential, BN Nanotubes, magnetization, Binding energy, adatom

1. Introduction

Recent years have witnessed great efforts being dedicated on two dimensional (2D) materials as inspired by the extensive interest and intriguing properties of graphene [1]. It is verified by many researchers and scientists that graphene sheet possesses covalently bonded honeycomb lattice which shows high stability and extraordinary properties [2], such as ambipolar effect, Klein tunneling, high electron mobility even at room temperature and anomalous quantum Hall effect [3]. Moreover, theoretical and experimental calculations on carbon nanotubes (CNTs) have shown excellent properties that make CNTs suitable for many proposed applications in different fields [3, 4]. The remarkable progress of graphene research has motivated scientists to explore other 2D materials such as phosphorene [5-7], MoS_2 [8] etc. Among these, boron nitride (BN) sheet has become very popular, because it shares the same honeycomb lattice structure as graphene. Using a chemical solution derived method single crystalline hexagonal BN and BN monoatomic sheet have successfully been synthesized [9]. Boron nitride nanotubes are basically semiconducting with wide band gap [10] and their electronic properties are independent of the chirality, tube diameter and of whether a nanotube is single walled or multiwalled [11]. Doping of various metallic species is a conventional method which shows capability to significantly enhance many of the physical properties of the most materials [12]. Recently adsorption of 5-fluorouracil molecule (5FU) into Al- and Ga- doped BNNTs are noticed to be thermodynamically stable.

*Co-Corresponding author: Tel: +923445490402
e-mail: imraniub86@gmail.com
Tel: +923457257132, Fax: +92-61-9210098
e-mail: anwarmanzoor@bzu.edu.pk

Additionally, 5FU depicts strong adsorption upon Al-doped BNNTs [13]. The germanium doped (Ge-doped) (8, 0) single-walled BNNTs are proved to be novel sensor for the detection of toxic pollutant in the atmosphere like carbon monoxide (CO) and nitric oxide (NO) [14]. Furthermore, doping of carbon (C) atoms into BNNTs could noticeably decrease the energy gap [15, 16] and such decrease is sensitively dependent upon the content of C atoms. Additionally, the effect of radial deformation on the bandgap tuning of single-walled (9, 0) and (5,5) BNNTs have also been investigated by applying a pressure of 10 GPa making it suitable for various device applications [17]. Subsequently, Han *et al.* developed a simple chemical route to coat BNNTs successfully with a conductive stannic oxide for possible sensor applications [18]. Experiments have shown that resistivity of the fluorinated BNNTs are about one third of that of pure BNNTs, which suggests that these materials may be important for applications in the future nanoscale electronic devices with tunable electrical properties [19]. It is note-worthy that uniformly doped BNNTs obtained through chemical modifications could be very effective for tailoring the electronic properties. Recent studies on the first-row adatom into different nanotubes like CNTs and SiC show the induce magnetism [20]. Also, first-row atoms do not exhibit cluster formation on the nanotube as noticed in the case of transition metals with high cohesive energy. In addition, adatoms to the first-row are inexpensive and less toxic as compared to transition metal-based magnetic materials. It is the main cause to choose light elements for magnetism and it has become a hot topic now-a-days [20]. More recently, Yasuhito Ohta [21] have studied BN cluster formation through density functional tight-binding

molecular dynamics and Peng Fu *et al.* [22] have investigated the hydrogen storage in BN systems.

In present study, BNNTs are adsorbed with various adatoms in first-row at five different initial sites namely; Axial B-N bond (AX), Zigzag B-N bond (ZG), Hexagonal site (HS), on top of Boron (B) and on top of Nitrogen (N) atoms as demonstrated in Fig. 1(a). This work analyzes the stability of these adatoms and provides a comprehensive study of magnetic properties of BNNTs in the presence of these adatoms at different sites on (8, 0) BNNTs. The results have been discussed on the basis of charge transfer and/or rearrangement due to different electronic configurations of adatoms and BN nanotubes and any hybridization between *s-p* or *p-p* orbitals of adatoms and B and/or N atoms.

2. Computational Method

Since many experiments have shown that BNNT prefers a zigzag orientation during the growth [16], so we focus our investigations on the zigzag BNNTs in (8, 0) configuration, which contains a total number of 96 atoms. All our calculations are carried out within the plane-wave density functional theory (DFT) by using the Vienna *ab initio* simulation package (VASP) [23, 24]. The generalized gradient approximation (GGA) with the Perdew Burke Ernzerhof (PBE) functionals and projector augmented wave (PAW) potentials are selected in all these calculations [25-27]. The periodic boundary condition is applied for BNNTs along the tube axis followed by a vacuum region of 14 Å between various tubes to make sure that there is no mutual interaction between BNNTs. In order to determine the equilibrium configuration of BNNTs, all the atomic coordinates together with supercells were fully relaxed using conjugate gradient (CG) method and Hellmann Feynman forces were kept smaller than 0.01 eV/Å. The convergence tests on BNNTs systems were performed for total energy with respect to the electron wavefunctions by expanding plane-waves with optimized cut-off energy of 400 eV. The k points were generated with $1 \times 1 \times 5$ grid based on Monkhorst pack (MP) scheme. The smearing width having value of 0.1 eV was used in DOS plots calculations to converge the system. In addition, the binding energy (ΔE_{ad}) of an adatom on (8, 0) BNNTs can be obtained using the following equation [22, 28 and 29]:

$$\Delta E_{ad} = E_{tot}(BNNT + adatom) - E_{tot}(BNNT) - E_{tot}(adatom)$$

where $E_{tot}(BNNT)$, $E_{tot}(adatom)$ and $E_{tot}(BNNT + adatom)$ are the total energies of BNNT, free isolated adatom and BNNT + adatom respectively.
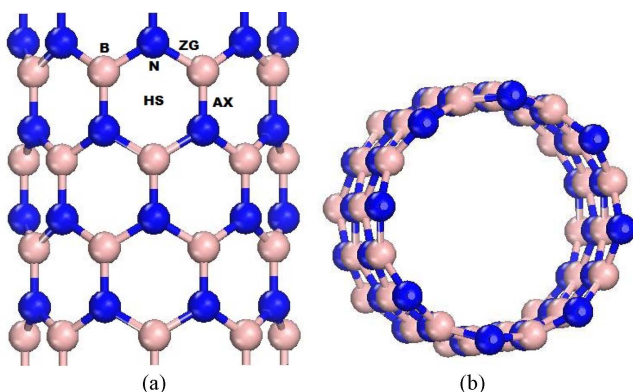
Fig. 1. (Color online) Optimized structure for the most stable configuration of first-row adatoms (a) on (8, 0) BNNTs; also illustrating completely the various initial sites of adatom adsorption chosen for calculations, and (b) (8, 0) zigzag single wall BNNTs: blue, pink and white colored atoms represent nitrogen, boron and hydrogen respectively.

3. Results and Discussion

3.1. Binding energy

To identify the lowest energetic configuration, five different initial sites were chosen for the incorporation of first-row adatoms, and binding energies of an adatom on (8, 0) BNNTs at each of these sites were determined separately. The results of these calculations are presented in Table 1. The smallest cell in BNNTs involves a rectangular unit containing two boron and two nitrogen atoms and repetition of such cell along the direction of circumference creates the primitive cell for zigzag BNNTs. The stable and fully optimized configuration (also illustrating various initial sites of adatom adsorption chosen for present DFT calculations) on (8, 0) BNNTs is displayed in Fig. 1(a), while Fig. 1(b) demonstrates (8, 0) zigzag configuration of BNNTs after full structural relaxation and optimization. Binding energies involved in these calculations due to hydrogen atoms attachments have been extracted to observe only the effect of adatoms adsorption.

Table 1. The binding energies and total magnetic moment of first-row adatoms on (8, 0) BNNTs.

First-row Adatom	Sites	ΔE_{ad} (eV)	Magnetic moment (μ_B)
Li	AX	−0.02	0.00
	B	0.98	−0.01
	HS	0.98	−0.03
	N	0.98	−0.01
	ZG	0.98	0.03
O	AX	−0.01	0.09
	B	−2.04	0.00
	HS	−2.04	0.00
	N	2.96	0.00
	ZG	−2.04	0.00
C	AX	0.96	0.00
	B	2.96	0.00
	HS	2.96	0.00
	N	1.96	2.02
	ZG	−0.04	0.00
Be	AX	0.98	0.00
	B	1.98	0.00
	HS	−1.05	1.93
	N	0.98	1.13
	ZG	−2.03	1.79
F	AX	2.90	0.16
	B	1.90	0.16
	HS	2.90	0.53
	N	−0.10	1.12
	ZG	2.90	1.13

For first-row atoms incorporated on the (8, 0) BNNTs, it is noticed that the most stable sites are different for different elements as obvious from Table 1. The Li as first-row adatom energetically prefers to stay at AX site as compared to all other sites since binding energy at AX site is negative (the lowest) indicating exothermic nature of the adsorption process. Similarly, O adatom prefers almost all chosen sites except on top of N atom, illustrating strong interaction when incorporated on top of B atom, at HS and ZG sites, while C adatoms energetically favor to bind themselves at zigzag sites, however adsorption of C adatom on top of N atom appears to be magnetically encouraging phenomenon. On the other hand, Be and F atoms exhibit strong binding at adsorption sites such as Be is most stable at ZG and HS sites while F prefers to be suitable on top of N atoms. It is notable that these adsorbed atoms on (8, 0) BNNTs possess lower energies. Oxygen adsorption requires the lowest energy which might be attributed to a significant transfer of charge from BNNTs to oxygen atom, whereas the highest binding energy for an adatom could be related with the structural deformation, which might occur during the adsorption process. Moreover, several other contributions such as the localized nature of occupied/unoccupied states near Fermi level of BN nanotubes, electronegativity's of first row adatoms with respect to neighboring B and N atoms etc. might also play dominant role in this adsorption process. As it is known that the electronegativity is responsible for the direction of charge transfer either from adatom toward nanotubes or from nanotubes toward adatom [28]. On the adsorption of an adatom, electrons transfer from an element of higher chemical potential to that of lower chemical potentials in order to balance the charge.

3.2. Magnetic properties

Several methods can be employed to study the magnetic coupling between similar and/or dissimilar atoms. In the present work we have chosen the same method which has been successfully employed by Wu *et al.* [30] in their research work. Figure 2 shows calculated density of states (DOS) at the AX site for all the studied adatoms. A deep observation of this plot depicts that the ferromagnetic (FM) coupling is detected only in F atoms adsorbed BNNTs present at AX sites close to B-N atoms. However, very weak magnetic behavior is noticeable on the adsorption of Li atoms on BNNTs as clear from Fig. 2. It is known that the spin-polarization mainly comes from *s-p* orbital hybridization of the atoms and so is responsible for the localized magnetic moments [9]. The interaction of F electron with those of B and/or N may cause localized magnetic moments. Moreover F also shows half
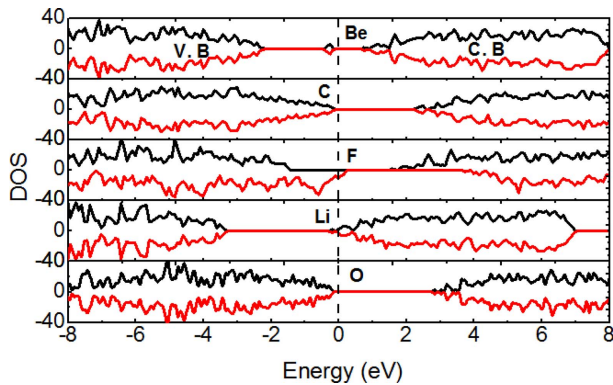
Fig. 2. (Color online) Spin polarized DOS of Be, C, F, Li and O. Fermi level is set at zero energy.

metallic characteristics with zero band gap due to shifting or rearrangement of charge at the Fermi level particularly the shifting of charge for spin down electrons from valence toward conduction band as obvious from Fig. 2. Be adatoms are creating localized impurity states in the band gap region. There is a clear spin polarization between DOS of the two spin channels at the Fermi level of adsorbed atoms on BNNTs, which shows magnetic behavior due to the majority and minority spin that crosses the Fermi level [31].

To check the effect of Li adatom on the magnetic behavior of BNNTs at all possible sites on the nanotubes, PDOS was calculated. The spin polarized PDOS of
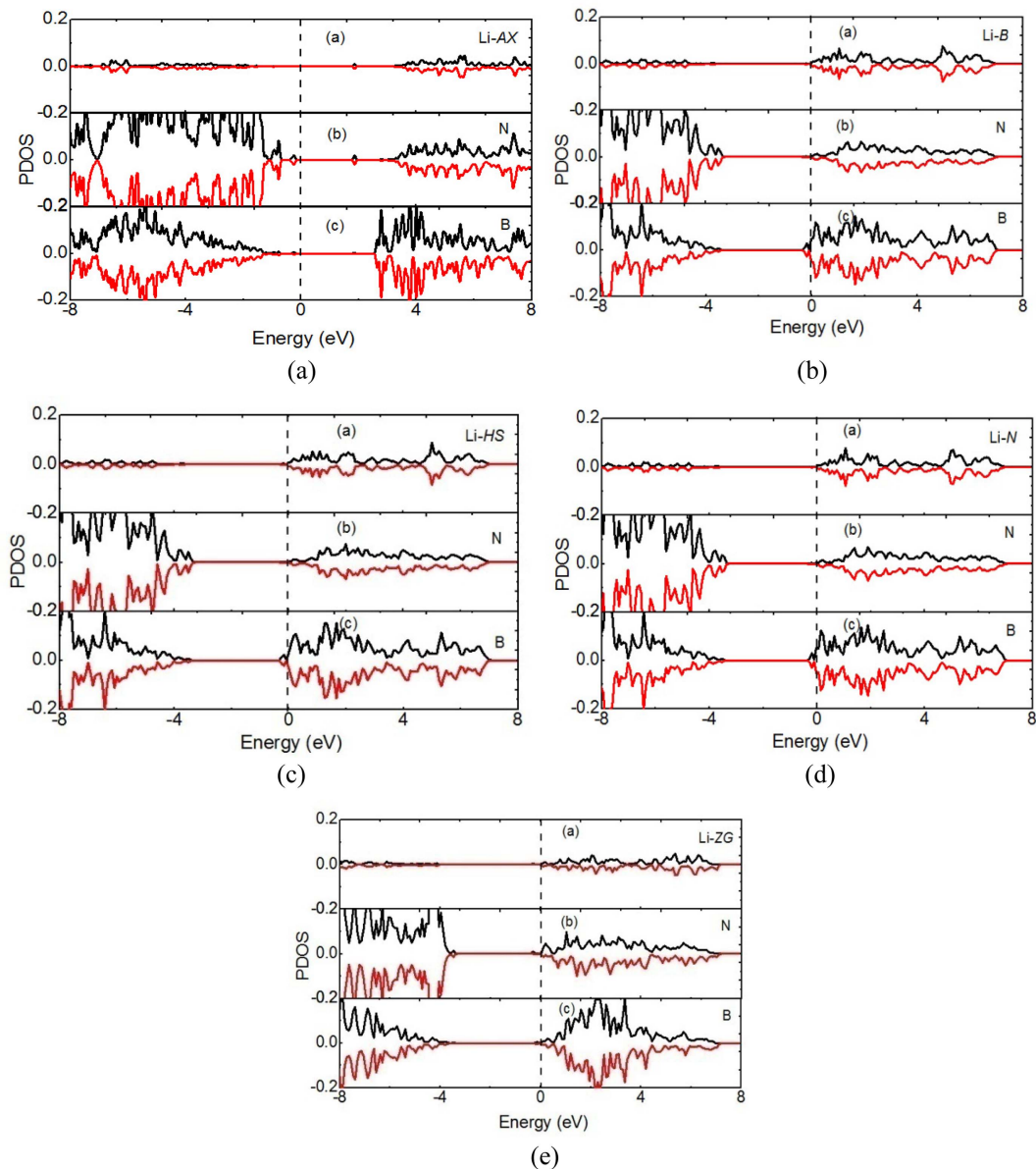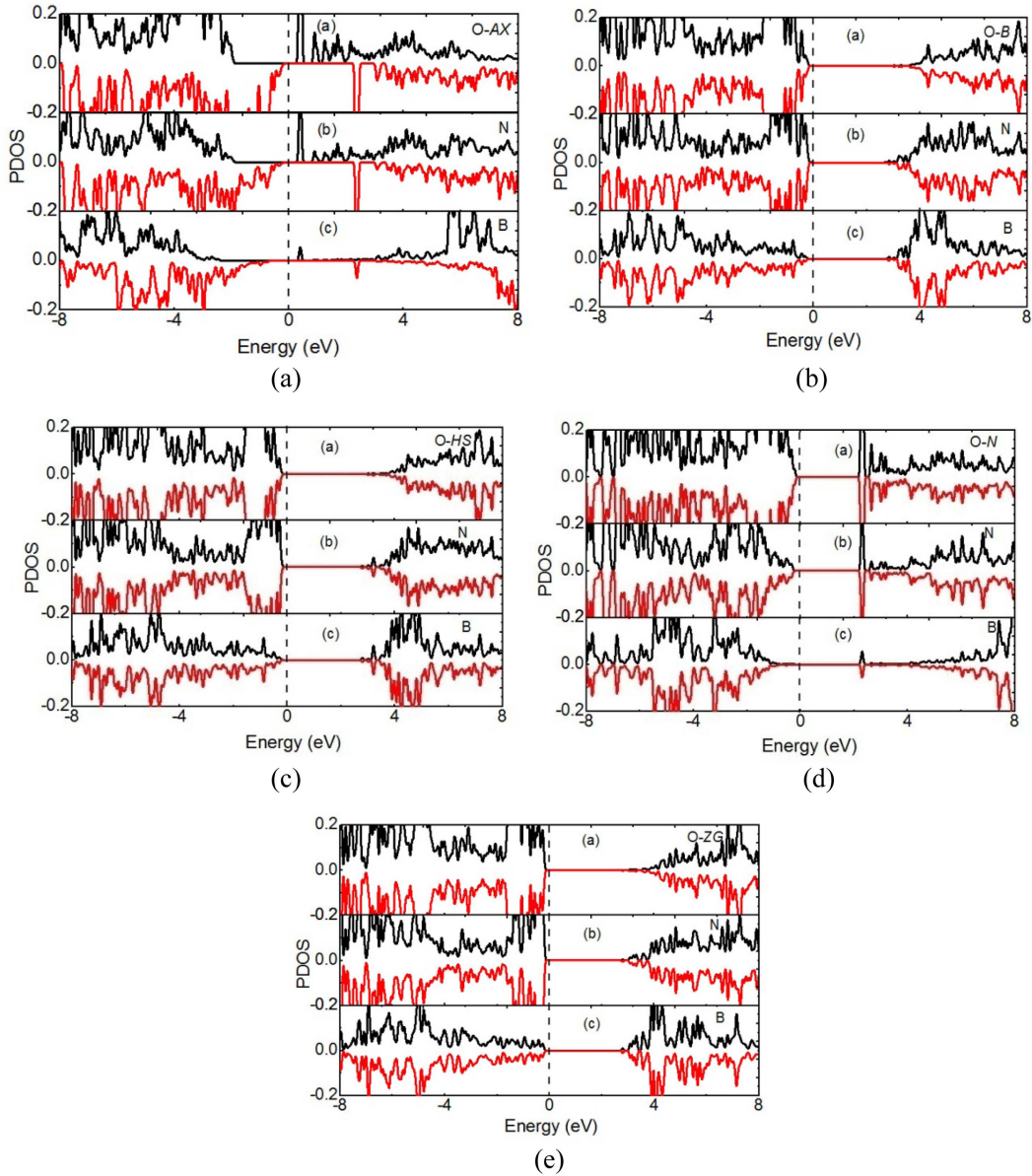

Fig. 3. (Color online) Spin polarized PDOS of component atoms when Li atom is adsorbed at (a) AX, (b) on top of B, (c) HS, (d) on top of N and (e) ZG sites.

component atoms when Li atom is adsorbed at various sites is shown in Fig. 3. It can be clearly seen that none of the doping sites except ZG are suitable for localized magnetic behavior in the BNNTs. Li adatoms at all other sites either create impurity states at the Fermi level and shift the conduction band minimum toward Fermi level or generate impurity levels in between the band gap region due to interaction of electrons in similar or different orbitals. None of the component elements except N at ZG site has contribution towards the localized net magnetic moment caused by the spin polarization of Li $2s^1$ and N $2p^3$ electrons particularly the spin down electrons. Such behavior results in weak magnetic nature of this system.

Furthermore, it can be observed that there is a significant band gap present between valance and conduction bands.

To explore the behavior of O adatom on BNNTs at various sites, PDOS was calculated and results are shown in Fig. 4. Although the PDOS of O adsorbed BNNTs is noticed to be significantly different from that of Li adatom BNNTs, however the net effect is magnetically equivalent. Results reveal that for O adatoms the axial adsorption sites are suitable for localized magnetic behavior in the BNNTs as some splitting of spin up and down states is observed for AX sites (Fig. 4a). This might be caused by the rearrangement of charges in the 2p states in the axial configuration due to the mutual interaction of
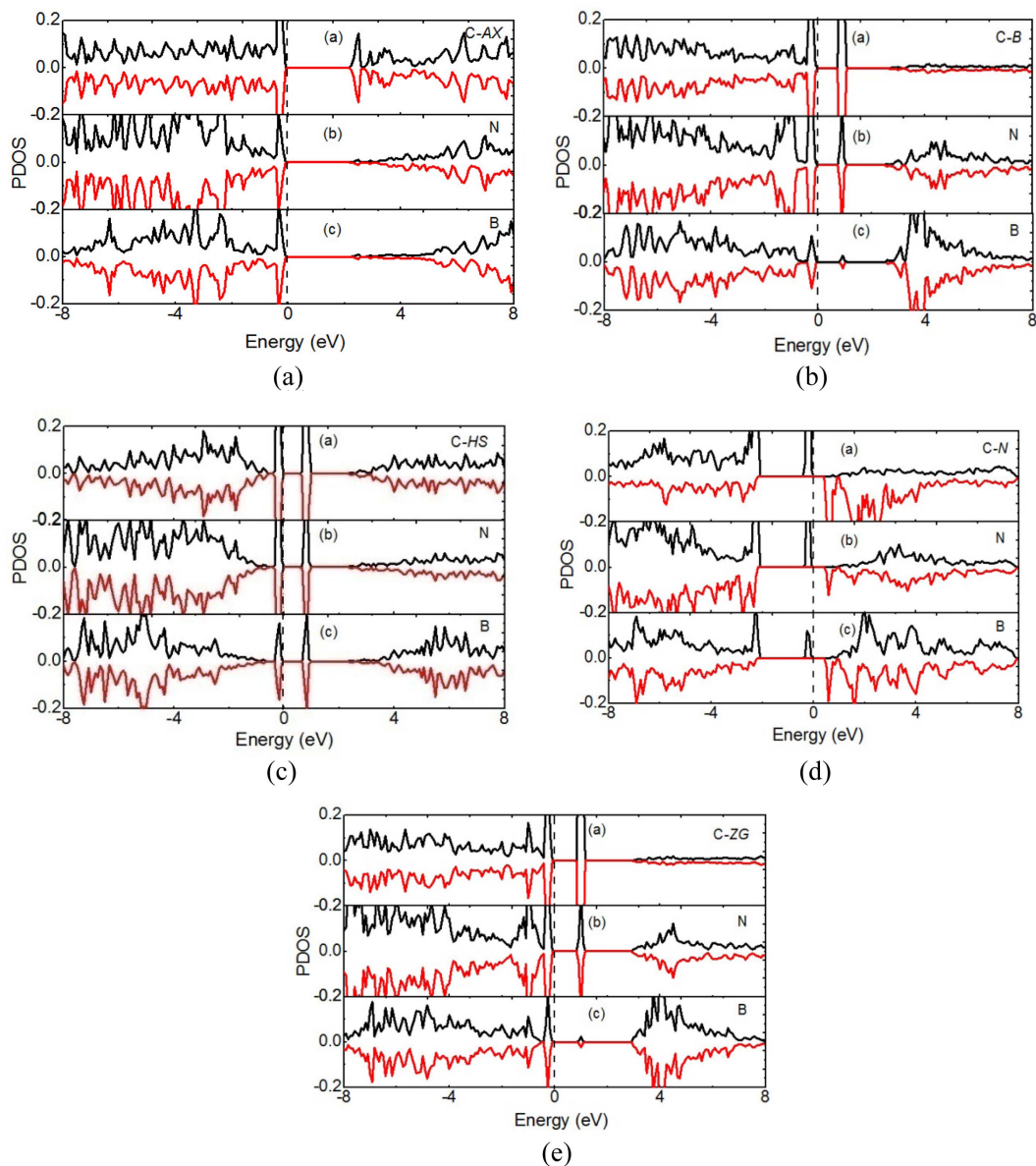

(a)

(b)

(c)

(d)

(e)

Fig. 4. (Color online) Spin polarized PDOS of component atoms when O atom is adsorbed at (a) AX, (b) on top of B, (c) HS, (d) on top of N and (e) ZG sites respectively.

both B and N with oxygen atom [9, 31]. Due to the interaction of 2p-electrons of both N and O, there is a shifting of charge toward conduction band leading some large peaks close to Fermi level. There is no other element which contributes towards the net magnetic moment resulting in non-magnetic nature of BNNTs. However these elements shift the Fermi level to the valence band edge and some of them create impurity states close to conduction band minimum (e.g. when O adatoms was placed on top of N atom in the BNNTs). Furthermore there still exists a large band gap between valance and conduction bands.

Figure 5 displays resultant spin polarized PDOS illustrating

the effect of C adatom on the magnetic behavior of BNNTs when adsorbed at various possible sites on the nanotubes. It is noticeable from Figs. 3 to 5 that the PDOS of C adatom on BNNTs is significantly different from that of O and Li adatoms. There is generation of sufficient amount of impurity/defect states at or close to Fermi level due to interaction of electrons of 2p-orbitals of C with that of B and N for both spins so the valance band shifts toward the Fermi level. This results in large PDOS peaks at or close to Fermi level. In addition, it is observed that when C adatom is adsorbed at top of N atom, there is a significant splitting of both the spin states in the case of both B and N atoms demonstrating the

Fig. 5. (Color online) Spin polarized PDOS of component atoms when C atom is adsorbed at (a) AX, (b) on top of B, (c) HS, (d) on top of N and (e) ZG sites respectively.
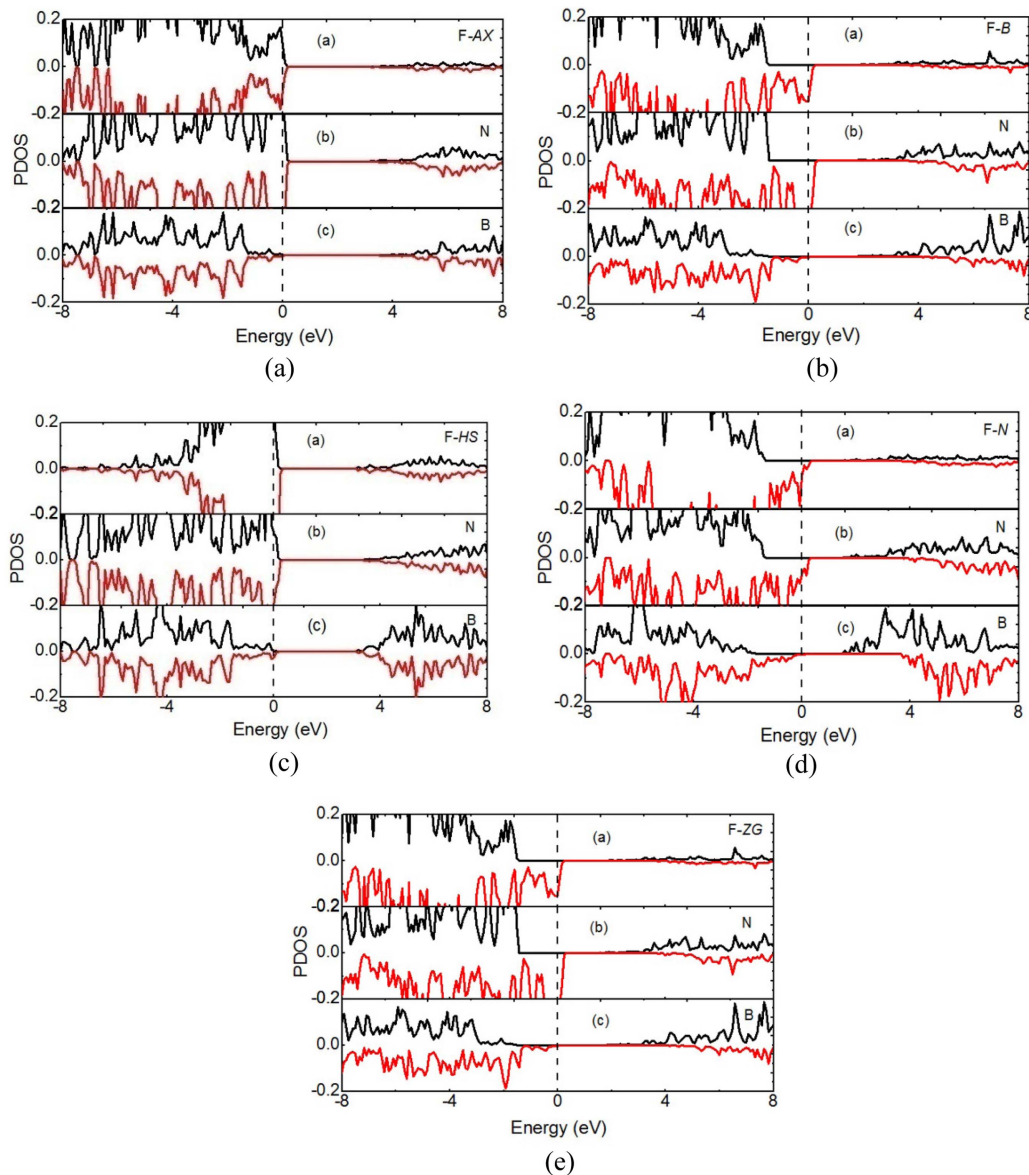
(a)

(b)

(c)

(d)

(e)
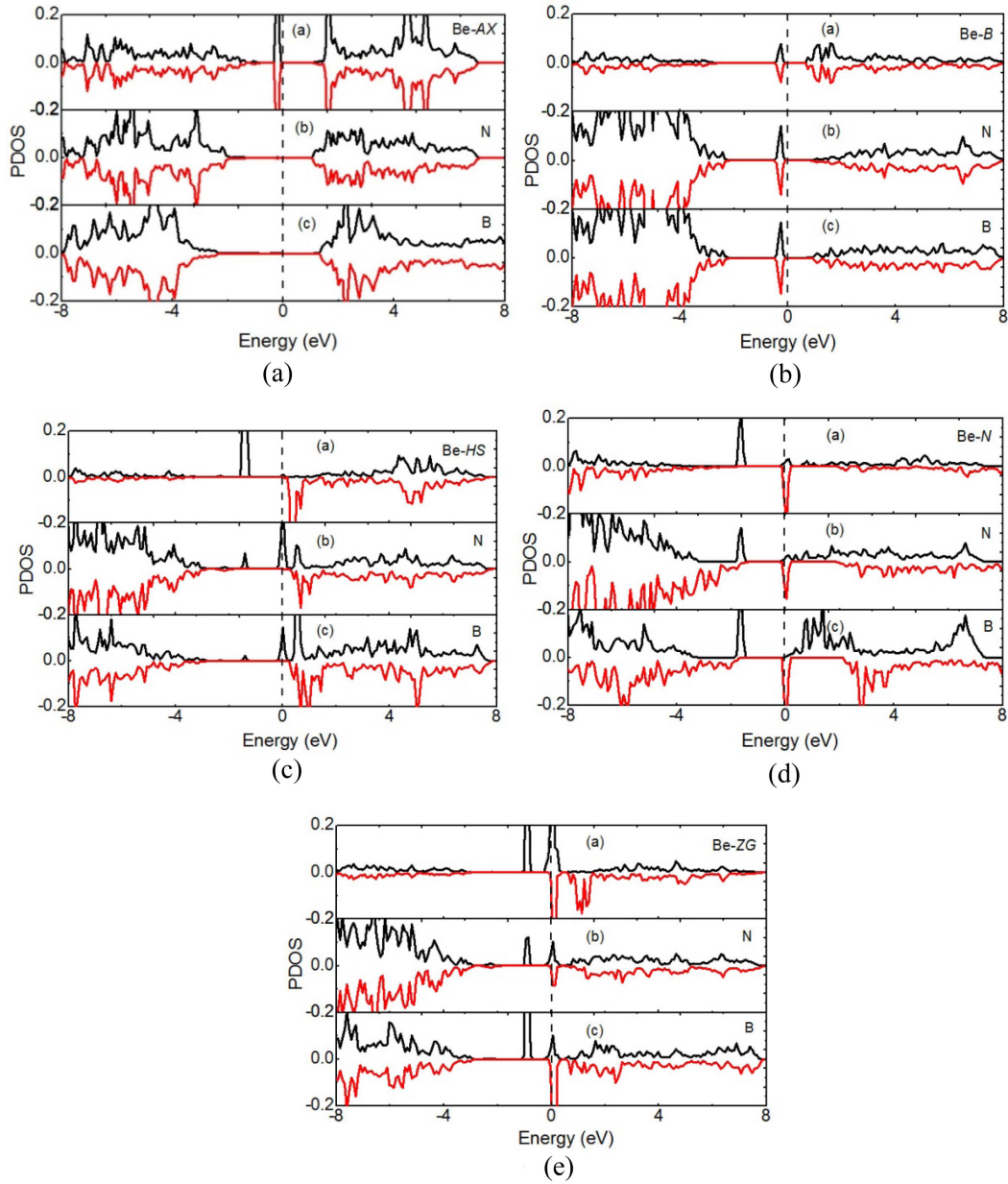
Fig. 6. (Color online) Spin polarized PDOS of component atoms when Be atom is adsorbed at (a) AX, (b) on top of B, (c) HS, (d) on top of N and (e) ZG sites respectively.

realignment of magnetic moments at these lattice sites. Due to the creation of states at or close to Fermi level, either there is no band gap or it is very small (0.7 eV) as compared to all other adatoms. Because of a lot of splitting of spin down states observed at B and N sites in conduction band, BNNTs depict localized magnetic behavior.

The spin polarized PDOS of component atoms when Be adatom is adsorbed at different possible sites is revealed in Fig. 6. It is seen that the adsorption of Be adatoms on BNNTs at AX and on top of B site just creates impurity states close to Fermi level along with shifting of conduction band minimum close to Fermi level as obvious from Fig. 6(a, b). However, for all other cases, splitting and rearrangement of states in the conduction band occurs for the both spin states and particularly in the spin down states. Therefore, it can be said that the adsorption of Be at HS, ZG and on top of N sites on BNNTs are suitable for induced local magnetic behavior as compared to AX and on top of B sites that show non-magnetic characteristics. Due to the shifting of conduction band minimum to the Fermi level, the calculated band gap is noticed to be 0 eV

(a)

(b)

(c)

(d)

(e)

Fig. 7. (Color online) Spin polarized PDOS of component atoms when F atom is adsorbed at (a) AX, (b) on top of B, (c) HS, (d) on top of N and (e) ZG sites respectively.

and lots of splitting states are observed in case of Be adsorption at HS, N and ZG sites near the Fermi level and in the conduction band that confirm the magnetic behavior of this element. Such change of behavior for Be adatom on BNNTs can be understood in terms of the mutual interactions between $2s$ and $2p$ orbitals of Be along with both B and N atoms, which looks to be responsible for the transfer/rearrangement of charge [31].

The calculated spin polarized PDOS of component atoms when F adatom is adsorbed at different sites is portrayed in Fig. 7. This figure clearly demonstrates the appearance of either weak or strong local magnetic effects observed at all the studied adsorption sites. So the PDOS

of F adatom on BNNTs are considerably different from that of Be and all other adatoms. It can be seen from Fig. 7(d, e) that for the F adatom on top of N and at ZG sites on BNNTs illustrates strong splitting of particularly spin down states for both B and N atoms so these sites are more suitable for locally induced magnetic behavior as compared to all other sites that show weak magnetic characteristics. The calculated band gap is very small and lots of splitting states are observed for all adsorption sites near the Fermi level that confirms the local magnetic behavior of this element. Such change of behavior for F adatoms on BNNTs can be explained on the basis of the mutual interaction between F $2p$ and $2p$ orbitals of both B

and N atoms and more contributions from N atoms, being responsible for the transfer/rearrangement of charge.

The FM coupling involving strong induced local magnetization is observed in case of Be, C and F atoms that are close to the neighboring atoms of boron and nitrogen [31]. This coupling is caused by orbital hybridization and the electrons rearrangements that occur between the adatoms and BNNTs [30]. In case of F adatoms, an acceptor level appears near the Fermi level close to the valence band edge, which is split into spin up and down states and ensures the local magnetization of the F adsorbed BNNTs. The PDOS indicates that the spin-polarization mainly comes from either *p-p* or *s-p* orbitals hybridization of the adatoms and both B and N atoms which appear to be responsible for the locally induced magnetic moments in adsorbed BNNTs [9].

4. Conclusions

Present study elaborates the method of locally inducing magnetization in non-magnetic BNNTs. For this purpose we have chosen five first-row adatoms to be adsorbed at various available sites on the (8, 0) BNNTs. All the calculations have been done with the help of VASP code employing GGA approximation and pseudo- potential technique. On the basis of these calculations several important conclusions can be made. It is found that for each adatom all sites have different binding energies and hence the sites are not equally preferable in terms of energy and stability of these adatoms. Among all of these adatoms, C adsorbed on top of N site and Be adatom at HS, ZG and on top of N sites locally induce significant magnetic moments in BNNTs due to *p-p* and *s-p* orbital hybridization. However, F adatom induces localized magnetic moments at all studied sites with ZG and on top of N sites are magnetically more preferred sites depicting strong spin polarization due to *p-p* orbital hybridization. All of these sites are magnetically favorable for F adatoms and so F can be considered as the most favorable candidate for inducing localized magnetization in BNNTs. Be can also be considered as good candidate due to its strong localized magnetic behavior at three of the studied adsorbing sites. Out of all the adatoms, Li and O show very low contribution towards the induction of localized magnetization hence cannot be used for this purpose.

References

[1] K. S. Novoselov, A. K. Geim, S. V. Morozov, D. Jiang, Y. Zhang, S. V. Dubonos, I. V. Grigorieva, and A. A. Firsov, Science **306**, 666 (2004).

[2] A. K. Geim, Science **324**, 1530 (2009).

[3] S. Iijima, Nature **354**, 56 (1991).

[4] R. S. Ruoff and D. C. Lorents, Carbon **33**, 925 (1995).

[5] Y. Q. Cai, K. Qingqing, Z. Gang, I. Boris, Yakobson, and W. Z. Yong, J. Am. Chem. Soc. **138**, 10199 (2016).

[6] Y. Q. Cai, Z. Gang, and W. Z. Yong, J. Am. Chem. Soc. **136**, 6269 (2014).

[7] Y. Q. Cai, K. Qingqing, Z. Gang, P. F. Yuan, B. S. Vivek, and W. Z. Yong, Adv. Funct. Mater. **25**, 2230 (2015).

[8] Y. Q. Cai, Z. Gang, and W. Z. Yong, Sci. Rep. **4**, 6677 (2014).

[9] W. Q. Han, L. Wu, Y. Zhu, K. Watanabe, and T. Taniguchi, App. Phys. Lett. **93**, 223103 (2008).

[10] X. Blase, A. Rubio, S. G. Louie, and M. L. Cohen, Euro. Phys. Lett. **28**, 335 (1994).

[11] A. Rubio, J. L. Corkill, and M. L. Cohen, Phys. Review B **49**, 5081 (1994).

[12] J. Zhaoa and R. H. Xieb, J. Nanosci. Nanotechnol. **3**, 459 (2003).

[13] S. Alireza, T. B. Mohammad, E. T. Lemeski, K. Sara, and B. Hanzaleh, J. Phys. and Chem. of Solids **86**, 57 (2015).

[14] W. Ruoxi, Z. Dongju, and L. Chengbu, Comp. Matr. Sci. **82**, 361 (2014).

[15] X. Blase, J. C. Charlier, A. D. Vita, and R. Car, Appl. Phys. A **68**, 293 (1999).

[16] D. Golberg, P. Dorozhkin, Y. Bando, M. Hasegawa, and Z.-C. Dong, Chem. Phys. Lett. **359**, 220 (2002).

[17] H. K. Yong, K. J. Chang, and S. G. Louie, Phys. Rev. B **63**, 205408 (2001).

[18] W. Q. Han and A. Zettl, J. Am. Chem. Soc. **125**, 2062 (2003).

[19] D. Golberg, W. Han, Y. Bando, L. Bourgeois, K. Kurashima, and T. Sato, J. Appl. Phys. **86**, 2364 (1999).

[20] Li. Feng, Z. Changwen, W. Peiji, and Li. Ping, Appl. Surf. Sci. **258**, 6621 (2012).

[21] Y. Ohta, Comp. Mater. Sci. **139**, 16 (2017).

[22] Fu. Peng, J. Wang, R. Jia, S. Bibi, R. I. Eglitis, and H. X. Zhang, Comp. Mater. Sci. **139**, 335 (2017).

[23] G. Kresse and J. Furthmüller, Phys. Rev. B **54**, 11169 (1996).

[24] G. Kresse and J. Furthmüller, Comp. Mater. Sci. **6**, 15 (1996).

[25] J. P. Perdew, K. Burke, and M. Ernzerhof, Phys. Rev. Lett. **77**, 3865 (1996).

[26] G. Kresse and J. Hafner, Phys. Rev. B **47**, 558 (1993).

[27] G. Kresse and D. Joubert, Phys. Rev. B **59**, 1758 (1999).

[28] S. Alireza, V. M. Ali, B. Mahsa, M. Anis, and S. Shamim, Physica B **430**, 20 (2013).

[29] A. P. Ali, S. Alireza, A. P. Amin, K. Yaser, and K. Soheila, Appl. Sur. Sci. **270**, 25 (2013).

[30] R. Q. Wu, G. W. Peng, L. Liu, and Y. P. Feng, Appl. Phys. Lett. **89**, 142501 (2006).

[31] R. Q. Wu, L. Liu, G. W. Peng, and Y. P. Feng, Appl. Phys. Lett. **86**, 122510 (2005).